

Two Novel D-A Type Polymers Employing 2,3-(4-(decyloxy)phenyl)quinoxaline as the Acceptor Unit, Thiophene and Selenophene as the Donor Units

Ya Luo¹, Jialei Zhang¹, Min Wang², Yan Zhang¹, Jinsheng Zhao^{1,*}, Chonggang Fu^{1,*}

¹Shandong Key Laboratory of Chemical Energy Storage and Novel Cell Technology, Liaocheng University, Liaocheng, 252059, P. R. China

²Liaocheng People's Hospital, Liaocheng, 252000, P. R. China

*E-mail: j.s.zhao@163.com, fuchonggang@lcu.edu.cn

Received: 12 November 2015 / Accepted: 28 November 2015 / Published: 1 January 2016

Two novel donor-acceptor-donor (D-A-D) type π -conjugated monomers, 2,3-bis(4-(decyloxy)phenyl)-5,8-di(thiophen-2-yl)quinoxaline (DPTQ) and 2,3-bis(4-(decyloxy)phenyl)-5,8-di(selenophen-2-yl)quinoxaline (DPSQ) were synthesized and be polymerized by electrochemical method. The structure-property relationships was indicated by the apparent difference in the electrochromic properties of the polymers. The properties of the polymer films were studied by cyclic voltammetry (CV), UV-Vis-IR, spectroelectrochemistry and scanning electron microscopy (SEM). The PDPTQ film showed a blue purple color at dedopped state and a transmissive light paleolivegreen color in the dopped state, with a bandgap of 1.62 eV. While, the PDPSQ film was saturated blue color in its dedopped state, and turned to transmissive light gray in the dopped state, and its bandgap is 1.53 eV. Both of the polymers showed excellent electroactivity and stability even up to 5000 cycles scans in cyclic voltammetry measurement. Moreover, the electrochromic parameters including the band gap, optical contrast, response time and coloration efficiency of two polymers were all reasonable and satisfactory. All of the excellent properties make these polymers good candidates for electrochromic device applications.

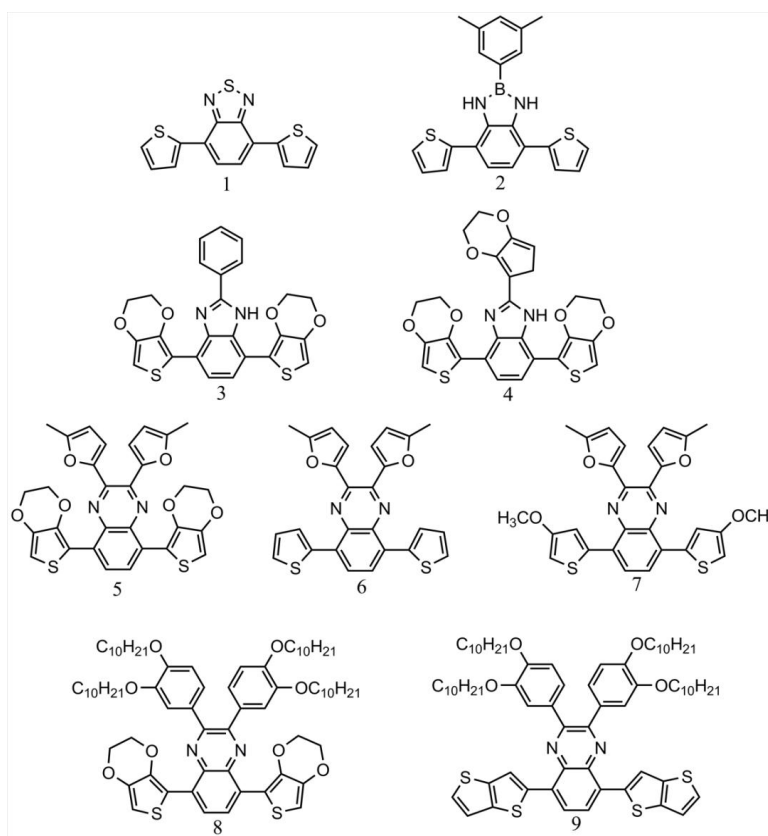
Keywords: Donor-acceptor-donor polymers; Quinoxaline; Electrochemical polymerization; Spectroelectrochemistry;

1. INTRODUCTION

Conjugated polymers have been shown an increasingly important area of research since the discovery of conductivity in polyacetylene upon doping [1]. Conjugated polymers showed great potentials in the fabrication of various types of devices such as transistors, sensing, emission,

patterning, charge storage, and photovoltaic and electrochromic devices [2-8]. Especially, conjugated polymers have shown important application prospects for the fabrication of innovative devices including non-emission displays, smart windows, mirrors and camouflage materials [9-13]. In recent years, polymer electrochromic materials have received more attentions than their inorganic partners due to their facile change of the nature of the polymer by structural modification. As an example, the introduction of alkyl chains to the polymer's backbone could improve the dissolution properties of the polymers, which is in favor of the preparation of large area electrochromic device by spraying method [14-17].

Recently, the adoption of alternating electron-rich and electron-deficient moieties in the backbone of polymers have become an attractive strategy for the preparation of low band gap cathodically coloring polymers.¹⁸ In the D-A type polymers, the broadening of the energy band was derived from the inter- and/or intra-molecular charge transfer (CT) interactions, and which can be used for the modification of the the absorption spectra and band gaps of the polymers [18].



Scheme 1. Some representative structure of D-A-D type conjugated systems.

Some of the conjugation systems were constructed by employing proper donor and acceptor units (Scheme 1).¹⁹⁻²³ Some of the reports on polymeric electrochromics containing benzothiadiazole derivatives as acceptor are reported from Toppare's laboratory (e.g., the monomer 3, 4 in Scheme 1)[19]. As another excellent acceptor-type unit, quinoxaline contained polymers have attracted increasing interesting. Our group has previously synthesized and investigated the electrochemical and optical properties of quinoxaline-based conjugated polymers which exhibited ambipolar property (e.g.,

the monomer 5, 6 and 7 in Scheme 1)[20]. As is known to all, quinoxaline-fused ring can ensure a rigid coplanar backbone and a highly extended π -electron system with strong π -stacking, which are crucial requirements for the high-performance electrochromic materials [21]. To obtain a quinoxaline soluble precursor backbone, the alkyl analogues substituents are necessary for the monomer 8, 9 in scheme 1)[23,23].

On the other hand, the changes in the electron-rich moieties could also be used for modifying the electrochromic characteristics of the materials in the case of the determined electron-deficient unit [18]. Thiophene and its derivatives are often employed as the electron donating units, and the electron donating strength of thiophene could be tuned by the introduction of different electron donating functional groups (e.g. alkyl and alkoxy) on its 3 and 4 positions[20]. Another simple method to modify the electrochromic properties of the polymers is replace the sulfur (S) atom in thiophene with a selenium (Se) atom. In thiophene containing polymers, the replacement of thiophene by selenophen could more easily lead to the red shift of the absorption spectra of the corresponding polymers [24]. Infact, some Se-containing units, such as selenophene, 3,4-propylenedioxyseleophene, and 3,4-ethylenedioxyseleophene have been used in the construction of electrochromic polymers with perfect electrochromic performance [25-27].

Taking into account the above considerations, two new D-A-D type monomers based on 2,3-bis(4-(decyloxy)phenyl)quinoxaline moiety as the acceptor units, thiophene and selenophene as the donor units were synthesized. And, the corresponding polymers were synthesized by the electrodeposition method. The influence of donor units on the electrochromic properties of the conjugated polymers was studied in detail. It was found that the replacement of thiophene by selenophen lead to the decrease in the band gaps of the polymers, as well as the changes concerning the electrochromic characteristics of the polymers. Furthermore, both of them exhibited excellent stabilities and fast switching times and low band-gap values, etc., which makes them promising candidates for electrochromic device applications.

2. EXPERIMENTAL

2.1. Materials

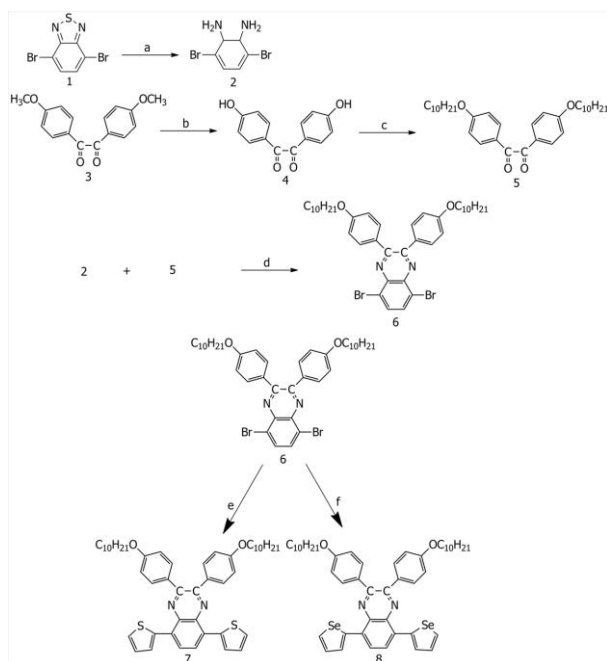
4,7-dibromo-2,1,3-benzothiadiazole and thiophene were purchased from Puyang Huicheng Electronic Material corp. Limited. 4,4'-Dimethoxybenzil and selenophene were obtained from J & K Chemical Technology. Sodium borohydride (NaBH_4 , 98%), anhydrous ethyl alcohol (EtOH, 99.9%), glacial acetic acid (HAc, 99.9%), hydrogen bromide solution (HBr, 48%), 1-Bromoocatane, tetrabutylammonium bromide, potassium carbonate, bis(triphenylphosphine) dichloropalladium ($\text{Pd}(\text{PPh}_3)_2\text{Cl}_2$), N,N-Dimethylformamide (DMF), toluene, tetrahydrofuran (THF), acetonitrile (ACN), dichloromethane (DCM), butyllithium and Tri-n-butyltin chloride were all purchased from Aladdin Reagent (Shanghai) corp. Limited. THF was dried and distilled over sodium in the presence of benzophenone be used as the indicator. Tetra-n-butylammonium hexafluorophosphate (TBAPF_6 , Alfa Aesar, 98%) was dried in vacuum at 60 °C for 24 hours before use. Indium-tin-oxide-coated (ITO)

glass (sheet resistance: $< 10 \Omega \square^{-1}$) was washed with ethanol, acetone and deionized water successively under ultrasonic, and dried under room temperature condition.

2.2. Equipments

Electrochemical synthesis and experiments were performed in a one-compartment cell with a CHI 760 C Electrochemical Analyzer under the control of a computer. A Varian Cary 5000 spectrophotometer connecting with a computer was used to record the UV-Vis-NIR spectra. Molecular fluorescence spectroscopy of the monomers were measured by Gangdong technologies F-380 fluorescence spectrometer. ^1H and ^{13}C NMR spectroscopy studies were recorded with a Varian AMX 400 spectrometer and chemical shifts were recorded in ppm units with tetramethylsilane (TMS) as the internal standard. The thickness of the polymer films were measured by AlphaStep® D-100 Stylus Profiler. Scanning electron microscopy (SEM) measurements were taken by using a Hitachi S-4800 thermionic field emission SEM. Digital photographs of the polymer films and device cell were taken by a Canon Power Shot A3000 IS digital camera.

2.3. Synthesis of DPTQ and DPSQ



Scheme 2. Synthetic route of the monomers. (a) NaBH_4 , EtOH, 0°C , 24 h; (b) HAc, HBr, reflux, 12 h; (c) 1-Bromooctane, tetrabutylammonium, Potassium carbonate, 120°C , 1.5 h; (d) HAc, reflux, 12 h; (e) $\text{Pd}(\text{PPh}_3)_2\text{Cl}_2$, toluene, tributyl(thiophen-2-yl)stannane; (f) $\text{Pd}(\text{PPh}_3)_2\text{Cl}_2$, toluene, tributyl(selenophen-2-yl)stannane, reflux, 24h.

As shown in Scheme 2, the synthetic route of the monomers as follows. The reduction of 4,7-dibromo-2,1,3-benzothiadiazole was achieved by using excess amount of NaBH_4 and produced 3,6-dibromo-1,2-phenylenediamine (2)[28]. 1,2-bis(4-methoxyphenyl)ethane-1,2-dione (3) was subjected

to substitution reaction with HBr and HAc was used as catalyst, the corresponding compound (4) was alkylated with decylbromide through a common procedure to gain another intermediate product 1,2-bis(4-(decyloxy)phenyl)ethane-1,2-dione (5)[29].

5,8-dibromo-2,3-bis(4-(decyloxy)phenyl)quinoxaline (6) was achieved by a simple condensation reaction between 2 and 5[30]. 1.0 g (3.76 mmol) of 2 and 1.96 g (3.76 mmol) of 5 were added into 250 ml of round-bottom flask filled with 100 ml of HAc. The mixture was refluxed at 120 °C and stirred magnetically for 12 hours. At the end of the reaction, cloudy mixture was observed. The solution was cooled to 0 °C and filtered. The separated solid was washed with EtOH several times and dried under vacuum oven to get a light yellow solid of compound 6. (2.3 g, 81%). ¹H NMR (CDCl₃, 400 MHz, ppm): δ_H = 7.85 (s, 2H, ArH), 7.65 (dd, 4H, ArH), 6.88 (dd, 4H, ArH), 3.99 (t, 4H), 1.86-1.71 (m, 4H), 1.52-1.01 (m, 28H), 0.88 (t, 6H). ¹³C NMR (CDCl₃, 101 MHz, ppm): δ = 160.76, 153.74, 139.34, 132.61, 131.84, 130.68, 123.72, 114.67, 68.42, 32.05, 29.56, 26.23, 22.81, 14.47 (see Supporting Information Fig. S1).

The monomers DPTQ, DPSQ were synthesized via Stille coupling reaction. Tributylstannane compounds were prepared according to previous literature methods [31]. The dibromoquinoxaline (6) was reacted with the corresponding tributylstannane compound under the catalysis of Pd(PPh₃)₂Cl₂ to obtain the target monomers DPTQ, DPSQ[28]. The detailed procedures are as follows: 3 g of compound 6 (4 mmol) and the excessive corresponding tributylstannane compounds (12 mmol) were dissolved in 80 ml of toluene, 0.14 g of Pd(PPh₃)₂Cl₂ (0.2 mmol) was also added in the solution. The reaction mixture was maintained refluxing under argon atmosphere for 24 h, and then cooled and concentrated on the rotary evaporator. The residue was purified by column chromatography on silica gel, in which n-hexane-dichloromethane (2:1, by volume) was as the eluent. The purified product DPTQ is yellow solid with 60% yield. ¹H NMR (CDCl₃, 400 MHz, ppm): δ_H = 8.10 (s, 2H, ArH), 7.85 (dd, 2H), 7.72 (d, 4H, ArH), 7.51 (dd, 2H), 7.18 (dd, 2H), 6.9 (d, 4H, ArH), 4.00 (t, 4H), 1.91-1.67 (m, 4H), 1.50-1.12 (m, 28H), 0.89 (t, 6H). ¹³C NMR (CDCl₃, 101 MHz, ppm): δ = 160.21, 151.51, 139.17, 137.20, 132.07, 131.02, 128.87, 125.64, 114.45, 68.30, 32.11, 29.64, 26.29, 22.88, 14.32 (see Supporting Information Fig. S2).

The crude production of DPSQ was purified by column chromatography on silica gel, in which n-hexane-dichloromethane (3:1, by volume) was the eluent. The purified product DPSQ is a red solid with 62% yield. ¹H NMR (CDCl₃, 400 MHz, ppm): δ_H = 8.21 (s, 4H), 8.07 (s, 2H), 7.65 (s, 4H, ArH), 7.44 (s, 2H), 6.93 (s, 4H, ArH), 4.01 (s, 4H), 1.82 (s, 4H), 1.29 (s, 28H), 0.89 (s, 6H). ¹³C NMR (CDCl₃, 101 MHz, ppm): δ = 160.16, 151.97, 142.09, 136.66, 136.12, 132.37, 130.98, 129.00, 127.01, 124.94, 114.34, 68.30, 32.15, 29.69, 26.33, 22.93, 14.36 (see Supporting Information Fig. S3).

2.4. Electrochemistry and Spectroelectrochemistry measurement

The equipment and the experimental procedures for the electrochemical deposition, electrochemical analysis and spectroelectrochemistry was described detailedly in our previously reports [20]. The electrodeposition and CV analysis were performed in ACN/DCM (3:1, by volume) solution containing 0.2 M tetrabutylammonium hexafluorophosphate (TBAPF₆) as a supporting

electrolyte with or without 0.005 M monomers. The pseudo reference electrode was calibrated externally using a 0.005 M solution of ferrocene (Fc/Fc^+) in ACN/DCM (3:1, by volume) solution containing 0.2 M TBAPF₆ as the electrolyte, and the half-wave potential ($E_{1/2}$) of Fc/Fc^+ measured was 0.55 V vs. Ag wire. And, the $E_{1/2}$ of Fc/Fc^+ measured in aforementioned solution containing 0.2 M TBAPF₆ was 0.4 V vs. SCE. In this case, the potential of Ag wire was assumed to be -0.15 V vs. SCE [20].

3. RESULTS AND DISCUSSION

3.1. Molecular fluorescence spectroscopy of the monomers

The UV-vis and photoluminescence (PL) spectra of the monomers in DMF are shown in Fig. 1 and the data are summarized in Table 1. The monomers in DMF solution exhibited UV-vis absorption peaks and fluorescence peaks at around 469, 550 nm for DPTQ and 519, 578 nm for DPSQ, respectively. The absorption and emission peaks could be assignable to the π - π^* transitions of the monomers. In both cases, the emission maxima experienced a red shift relative to their corresponding absorption maxima, indicating a Stokes shift values of 81 and 59 nm for DPTQ and DPSQ, respectively. The Stokes shift is an indication of the energy loss resulting from the vibrational relaxation of the excited states [32]. The emission maxima and absorption maxima of DPSQ exhibits a red shift compare with the corresponding values of DPTQ, owing to the electron donating ability of selenophene group is little stronger than that of thiophene group. Both of the monomers exhibited good fluorescence character in the visible region.

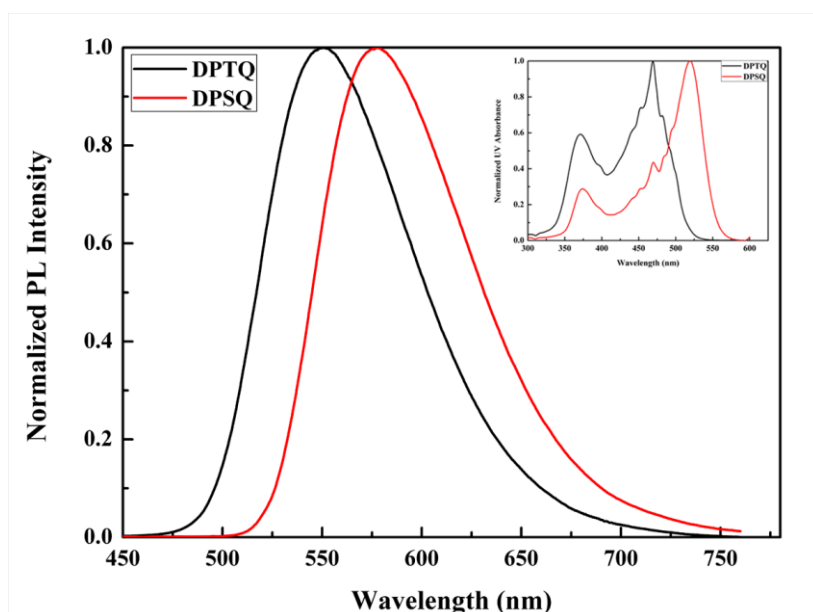


Figure 1. Normalized photoluminescence (PL) spectra of monomers of DPTQ and DPSQ. Inset: Normalized absorbance spectra of monomers of DPTQ and DPSQ.

3.2. Electrochemistry

The respective polymers were prepared by the electrochemical synthesis method, for this purpose, the monomers were dissolved in a mixture of DCM and ACN (3:1, by volume) solution containing 0.2 M TBAPF₆ as the supporting electrolyte. Fig. 2 shows the anodic electropolymerization of the monomers by CV method in the presence of a 0.005 M solution of DPTQ or DPSQ in the mixed solvent containing supporting electrolyte. As shown in Fig.2, the onset oxidation potentials (E_{onset}) of DPTQ and DPSQ are 1.09 V and 1.01 V, respectively. The E_{onset} of the latter monomer is slightly lower than that of the former one, which might be due to the more electron-rich characteristics of the selenophene unit than that of thiophene unit [33]. As the repetitive CV scans, the generation of new redox couples and the raise in the current amplitudes in the CV curves indicate the formation of the polymers on the working electrodes. As shown in Fig. 2a, the DPTQ CV profile show only one oxidation peaks at around 0.74 V, while the corresponding cathodic waves are 0.56 V. The CV profile of DPSQ shows a cathodic peak at around 0.8 V and a weak oxidation peak at around 0.85 V (Fig. 2b). The different locations and different appearance of the redox peaks of the polymers reveal the influence made by different electron-rich groups.

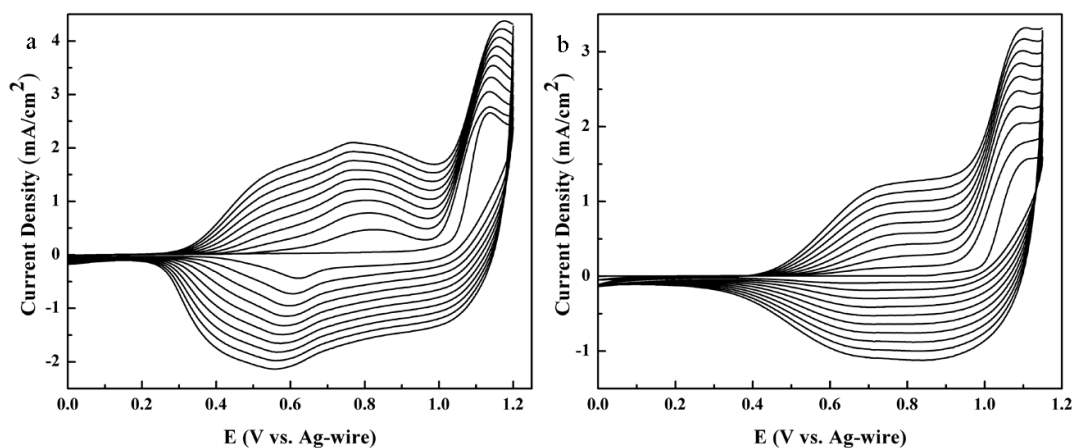


Figure 2. Cyclic voltammogram curves of (a) DPTQ (b) DPSQ in CAN/DCM (3:1, by volume) containing 0.2 M TBAPF₆ solutions at a scan rate of 100 mV s⁻¹.

The corresponding polymer films were deposited by CV over 3 cycles on the working electrode (area = 0.0628 cm²). Electrochemical behaviors of two deposited polymers were investigated at different scan rates in monomer free electrolyte. As shown in Fig.3, both of the polymers exhibit well defined redox peaks, and the $E_{1/2}$ of PDPTQ and PDPSQ were observed at 0.7 V verse Ag/Ag⁺ ($E_{\text{ox/p}}=0.78$, $E_{\text{red/p}}=0.62$ V verse Ag/Ag⁺ at the scan rate of 100 mV s⁻¹) and 0.87 V verse Ag/Ag⁺ ($E_{\text{ox/p}}=0.87$, $E_{\text{red/p}}=0.7$ V verse Ag/Ag⁺ at the scan rate of 100 mV s⁻¹), respectively. The reason for the different $E_{1/2}$ values are attributed to the differences of the donor unit of the monomer[33]. As shown in Fig. 3a, PDPTQ film exhibits a redox process between 0.62 and 0.78 V (p-doping/dedoping), but there is no obvious n-doping/dedoping peaks in the polymer, which suggests that PDPTQ is a p-type

conjugated polymer. Polymeric electrochromics with n-doping ability are limited in the literature because of the strict requirement for matching between the electron-rich unit and the electron-deficient unit. This phenomenon is also observed in the other polymer PDPSQ and similar conclusion can be obtained (Fig. 3b). Fig. 3c, shows the scan rate dependence of the anodic and cathodic peak currents, which shows a liner dependence as a function of the scan rate of the PDPTQ during the p-doping/dedoping process. It demonstrated that the film were well adhered on the surface of platinum wire and the electrochemical processes are non-diffusion-controlled and, as shown in Fig. 3a, are quasi-reversible. The other polymer PDPSQ also present the similar linear relationships between the scan rates and the peak current densities (Fig. 3d).

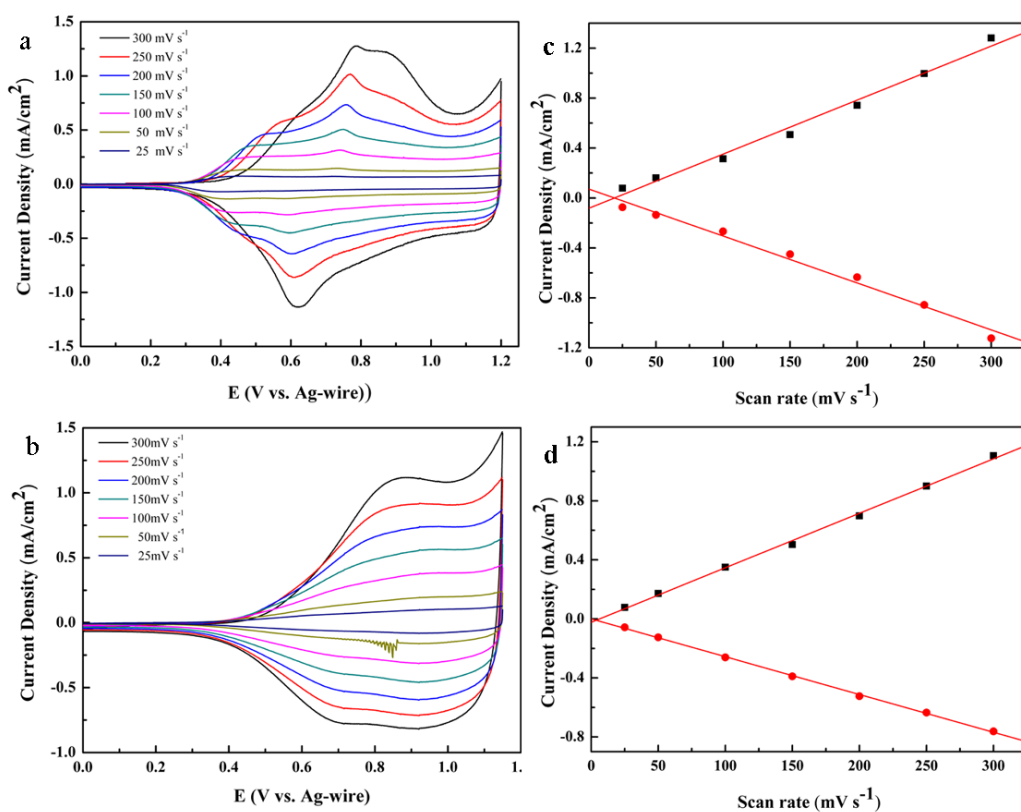


Figure 3. (a) and (b): CV curves of PDPTQ and PDPSQ at different scan rates between 25 and 300 mV s^{-1} in the monomer-free 0.2 M TBAPF₆/ACN/DCM solution, respectively; (c) and (d): the linearity of the current density versus voltage scan rate of the p-doping/dedoping process for PDPTQ and PDPSQ, respectively.

3.3. Morphology

The films were prepared at a given potential on ITO electrode in the ACN/DCM solution containing the supporting electrolyte and the respective monomers, and the polymer was dedoped in monomer free electrolyte before characterization. The thickness of polymers films were measured by step profiler. As can be seen from Fig. 4, the thickness of PDPTQ is approximate 440 nm and PDPSQ is 389 nm, the surface morphologies of PDPSQ is rougher than that of PDPTQ. The SEM images of

two polymer films are shown in Fig. 5. The PDPTQ film exhibits an accumulation state of clusters of random granules and shows tiny pores structure (Fig. 5a). As for PDPSQ film, it exhibits a coralloid structure with many relative huge pore canal (Fig. 5b). There are obvious differences in the structure of the two polymers, presenting the difference aggregation structures of the polymers, which was strongly dependant on the structures of the monomers.

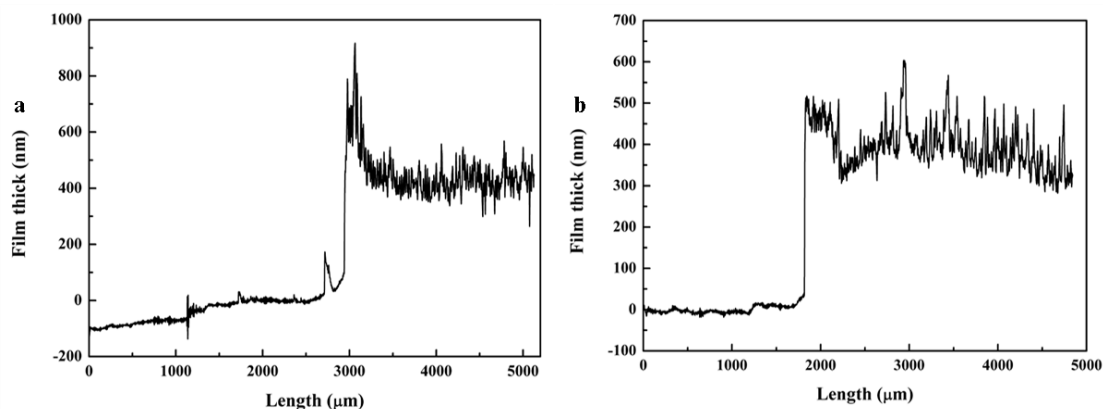


Figure 4. The thickness of the polymers films: (a) PDPTQ and (b) PDPSQ deposited potentiostatically onto ITO electrode.

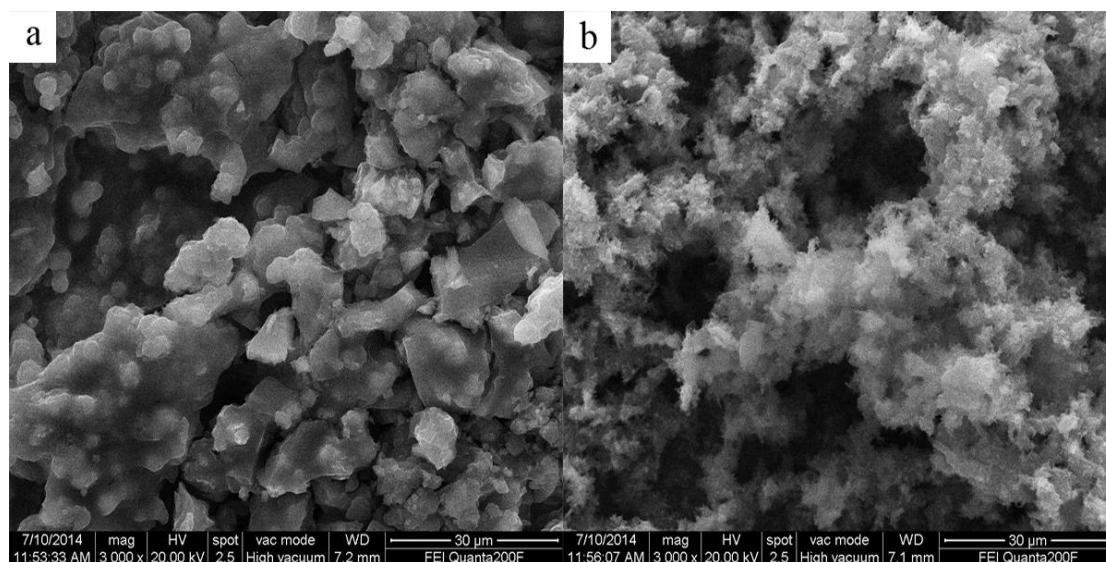


Figure 5. SEM images of (a) PDPTQ and (b) PDPSQ deposited potentiostatically onto ITO electrode.

3.4. Optical properties of the monomers and films.

The UV-Vis spectra of two monomers (dissolved in DCM) and the dedoped polymer films are shown in Fig. 6. The PDPTQ, PDPSQ films were electrodeposited onto ITO electrode with the same polymerization charge of 2.0×10^{-2} C at 1.2 V and 1.15 V, respectively. The experiments were performed in the same electrolytic medium ACN/DCM (3:1, by volume) solution containing 0.2 M

TBAPF₆ as a supporting electrolyte and 0.005 M monomers. After that, electrochemical dedoping was carried out at 0 V and then be washed with ACN/DCM solution for 3 times.

Both of the monomers have two obvious absorption bands with the maximum peaks value of 313 and 405 nm for DPTQ and 321 and 414 nm for DPSQ, respectively. DPSQ has 8-9 nm bathochromic shifts for both of the absorption bands than that of the monomer DPTQ, which might be attributed to the stronger electron-donating ability of the selenophene unit than that of thiophene unit. The red shift trend is more pronounced for the corresponding polymers, there is a 72 nm bathochromic shift for the low energy absorption peak of the PDPSQ compared with that of the PDPTQ polymer. Moreover, both of the polymers exhibit a red shift compared to the corresponding monomers, as shown in Fig. 6, which indicates the extension of the conjugation length due to the growth of the molecular chain [27].

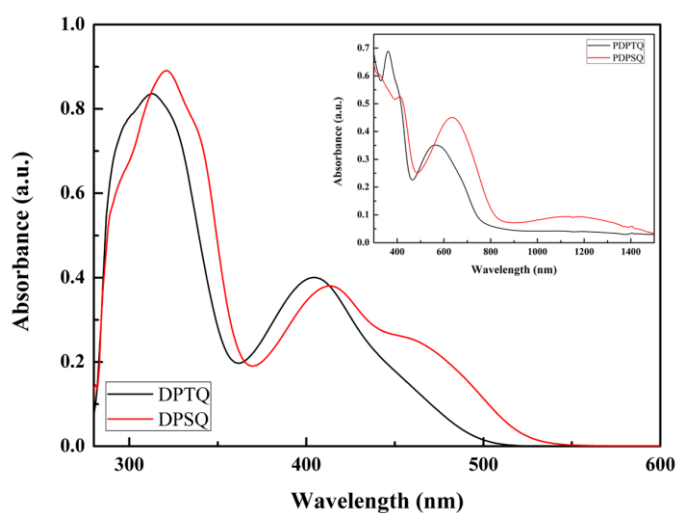


Figure 6. UV-vis absorption spectra of DPTQ and DPSQ. inset: absorption spectrum of the corresponding polymers.

Table 1. The onset oxidation potential (E_{onset}), maximum absorption wavelength (λ_{max}), absorption onsets wavelength (λ_{onset}), HOMO and LUMO energy levels and optical band gap (E_g).

Compounds	E_{onset} , vs. (Ag-wire) (V)	λ_{onset} (nm)	λ_{max} (nm)	HOMO ^b (ev)	LUMO ^c (ev)	E_g^a (ev)	HOMO [*] (ev)	LUMO [*] (ev)	E_g^* (ev)
DPTQ	1.09	497	404	-5.45	-2.95	2.5	-5.37	-2.4	2.97
DPSQ	1.01	525	414	-5.4	-3.04	2.36	-5.25	-2.46	2.79
PDPTQ	0.32	766	571	-4.57	-2.95	1.62	-	-	-
PDPSQ	0.41	810	636	-4.66	-3.13	1.53	-	-	-
PDOPEQ [*]	-	-	-	-	-	1.45	-	-	-
PQTT [*]	-	-	-	-	-	1.3	-	-	-

^a Calculated from the low energy absorption edges (λ_{onset}), $E_g = 1240/\lambda_{\text{onset}}$.

^b HOMO = $-(E_{\text{onset}} + 4.4)$ (E_{onset} vs. SCE).

^c Calculated by the subtraction of the optical band gap (E_g) from the HOMO level.

^d Absorption maximum from UV-vis spectrum in DMF solution.

^c PL emission maximum of in DMF solution . Absorption maximum was taken as the excitation wavelength (λ_{ex}).

HOMO*, LUMO*, E_g^* were calculated by DFT calculations.

PDOPEQ* Data were taken from Ref.³⁰

PQTT* Data were taken from Ref.²³

Table 1 clearly summarizes the onset oxidation potential values (E_{onset}), low energy absorption edges (λ_{onset}), maximum absorption wavelength (λ_{max}), optical band gap (E_g) values, HOMO and LUMO energy levels of the monomers and the corresponding polymers calculated based on the experiment data. The parameters including E_g^* , HOMO* and LUMO* energy levels of the monomers were calculated by Gaussian 09 programs based on density functional theory (DFT)[34].

The data from the quantum chemical calculations can be used with the experimental results for the investigation of the structure-property relationships. Optimized ground-state geometries were calculated on the DFT level taking advantage of the Gaussian 09 programs. As seen from the HOMO and LUMO electron distribution map (Fig.7), the molecular orbital of the monomers largely delocalized on the aromatic rings, no distinct contribution of the external O atoms or adjacent C atoms is observed. Hence, the alkoxy substituent mainly increase the solubility of the monomer and the corresponding polymer and no significant electron donating function in this study was observed. The optimized conformation also shows that alkoxy substituents influence the planarity of the central acceptor unit and donor unit to some degree. Steric hindrance result from alkoxy substituents probably decreased the population of the quinoxaline electronic configuration and weaken the intermolecular charge transfer, and ultimately affect the optical properties of the polymer.

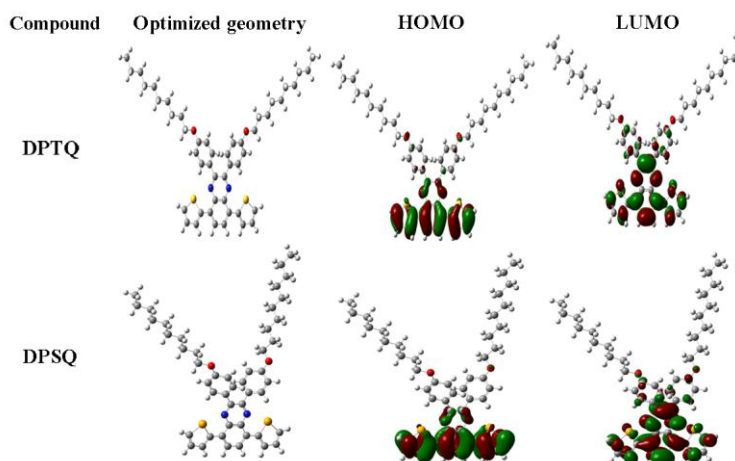


Figure 7. The optimized geometries and the molecular orbital surfaces of the HOMOs and LUMOs for DPTQ and DPSQ.

As the theoretical calculation results shown in Table 1, the monomer DPSQ has a higher HOMO level and a lower LUMO level than that of the corresponding monomer DPTQ, which led to the lower lower bandgap of the DPSQ than that of DPTQ. At the same time, the optical bandgaps of

the monomers were also calculated from the low energy absorption edges (λ_{onset}) ($E_g = 1240/\lambda_{\text{onset}}$), and the results are in good agreement with theoretical calculations. Furthermore, calculated values were found to be higher than the values from experimentally data, which probably resulted from the calculation models differences and the experimental condition discrepancies between the actual and the ideal conditions. According to previous reports, in the D-A-D type monomers, the results of the intermolecular charge transfer make the monomer has an ionization potential closer to donor and an electron affinity closer to the acceptor [33].

3.5. Spectroelectrochemical properties of the polymer films

Spectroelectrochemical measurements were undertaken for the acquiring the changes in the absorption spectra due to changes in electronic structure of the conjugated polymer as the voltage applied on the polymer film increased gradually. The polymer films for these studies are prepared by the potentiostatic polymerization method on ITO electrode (film forming area: 0.9 cm \times 3.0 cm) with an polymerization charge of 1.5×10^{-2} C. The joint utilization of the CHI760 C potentiostat and the UV-Vis-NIR spectrometer was applied for the record of the absorption of the polymer films via gradually increasing applied potential between 0 V and 1.2 V for PDPTQ, 0 V and 1.15 V for PDPSQ. Both polymers display similar absorption in the reduced state, with two distinct absorption bands, with one in the UV region and another in the visible region. And, the low energy peak for PDPTQ, which is centered at 563 nm, originating from the D-A interaction, absorbs the yellow, red, green light and also partial blue color, let the polymer film display a blue purple color in the reduced state (Fig. 8a)[18]. For PDPSQ polymer, two well defined absorption peaks with comparable intensities are located at 410 and 635 nm, respectively, with a regular valley centered at 486 nm, allowing the blue light to penetrate, thus showing a saturated blue color in the neutral state.

Upon oxidation of PDPTQ, the intensities of the transition absorption decrease and typical evolution of peaks around 792 nm and 1500 nm occurs corresponding to the polaronic and the bipolaronic bands. Upon fully oxidation a transmissive light paleolivegreen color was observed at 1.2 V for PDPTQ. Be similar with PDPTQ film, the PDPSQ film represents blue color with an absorption band at 635 nm in the visible region due to the π - π^* transition at the neutral state. With the doping of the PDPSQ film, the π - π^* transition peak decreased with the increase of the applied potentials and new absorption bands centered at 924 nm and 1563 nm evolved due to the formation of charge carriers on the polymer backbone named polarons (radical cation) and bipolarons (dication). At the full oxidation state, the π - π^* transition absorption bands depleted with a tiny absorption was observed in the visible region, result in a highly transmissive light gray color. Out of our expectations, no apparent n-doping processes was observed for both of the D-A-D type polymers, the reason for which might be the absence of the ideal match between the donor and the acceptor unit as seen in the ambipolar donor-acceptor polymers, such as PDOPEQ, in which 3,4-ethylenedioxythiophene, having a more strong electron donating ability than thiophene, was used as the donor unit in the D-A-D type polymer[30].

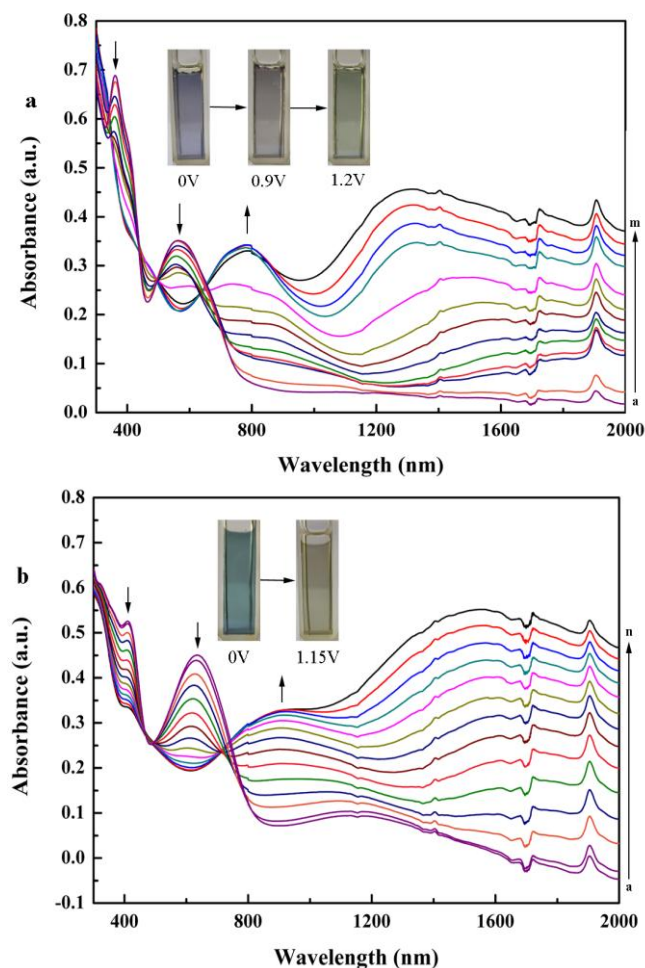


Figure 8. (a) p-doping: Spectroelectrochemistry of PDPTQ films on ITO electrode as applied potentials between 0 V and 1.2 V in the monomer-free 0.2 M TBAPF₆/ACN/DCM solution: (a) 0.0, (b) 0.2, (c) 0.4, (d) 0.42, (e) 0.45, (f) 0.5, (g) 0.6, (h) 0.7, (i) 0.8, (j) 0.9, (k) 1.0, (l) 1.1, (m) 1.2. (b) p-doping: Spectroelectrochemistry of PDPSQ films on ITO electrode as applied potentials between 0 V and 1.15 V in the monomer-free 0.2 M TBAPF₆/ACN/DCM solution: (a) 0.0, (b) 0.5, (c) 0.4, (d) 0.65, (e) 0.7, (f) 0.75, (g) 0.8, (h) 0.85, (i) 0.9, (j) 0.95, (k) 1.0, (l) 1.05, (m) 1.1, (n) 1.15.

3.6. Kinetic Studies

Response time and contrast are two important indicators of the performance of the electrochromic materials, which can be evaluated by the multi-step potential method linked with the optical spectroscopy method. The polymerization charge was 1.5×10^{-2} C on the ITO-coated glass with the active area of $0.9 \text{ cm} \times 3.0 \text{ cm}$.

The optical contrast is considered as the transmittance distinction between the dedoped and doped state at a specified wavelength. Response time was calculated based on the time required for achieving 95% of a full transition from dedoped to doped states. Fig. 9 exhibited the optical contrasts of two D-A type polymers at different wavelengths. After continuous switching for 300 s, no apparent loss in optical contrasts was observed, this suggested the high stabilities of two polymer

films. The optical contrasts and the response time times from reduced to oxidized state of the two polymer films at different wavelengths were summarized in Table 2. As shown in Fig.9 (Fig. 9a for PDPTQ and Fig. 9b for PDPSQ), both polymers showed moderate optical contrasts in the visible region with fast response times. It is noteworthy that both of the polymer films possess outstanding optical contrast (72% at 1500 nm for PDPTQ and 60% at 1500 nm for PDPSQ) in the NIR region, which is a very important property for some NIR applications, e.g. as camouflage coatings in military field. For comparison purpose, the switching properties of two structurally similar polymers, such as PDOPEQ and PQTT, were also included in Table 2 [30,23], from which it can be seen that PDPTQ and PDPSQ exhibited comparable performances in view of the switching properties, which make them promising candidates as electrochromic materials.

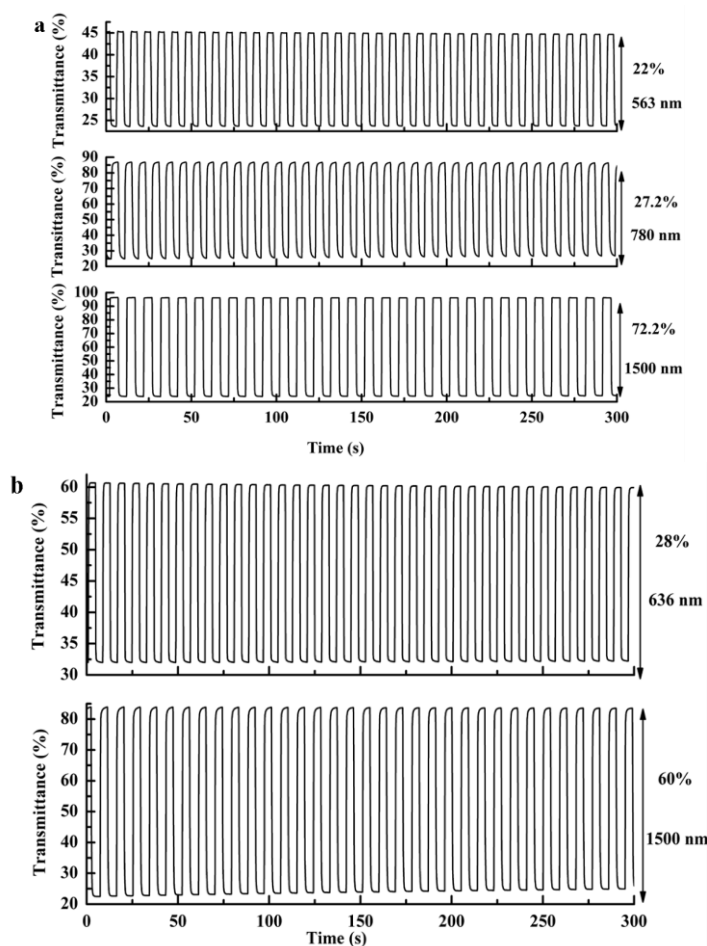


Figure 9. (a) Percent transmittance change monitored at 563, 780 and 1500 nm for PDPTQ between 0 V and 1.2 V. (b) Percent transmittance change monitored at 636 and 1500 nm for PDPSQ between 0 V and 1.15 V.

The coloration efficiency (*CE*) is also an important characteristic for the electrochromic materials. It can be calculate by the equations as follows[34]:

$$\Delta OD = \lg\left(\frac{T_b}{T_c}\right) \text{ and } \eta = \frac{\Delta OD}{\Delta Q}$$

Where T_b and T_c represent the transmittances before and after coloration. ΔOD is the change of the optical density, which is proportional to the amount of created color centers. η denotes the coloration efficiency (CE). ΔQ is the amount of injected charge per unit sample area. The CE of PDPTQ film was calculated to be $200 \text{ cm}^2 \text{ C}^{-1}$ at 563 nm, $71.7 \text{ cm}^2 \text{ C}^{-1}$ at 780 nm, and $218.2 \text{ cm}^2 \text{ C}^{-1}$ at 1500 nm. As for PDPSQ, the data of CE for which calculated by the equations mentioned above were $210.5 \text{ cm}^2 \text{ C}^{-1}$ at 636 nm and $366.7 \text{ cm}^2 \text{ C}^{-1}$ at 1500 nm. It is apparent that the Se atom containing polymer PDPSQ has a much higher CE value than that of the polymer PDPTQ.

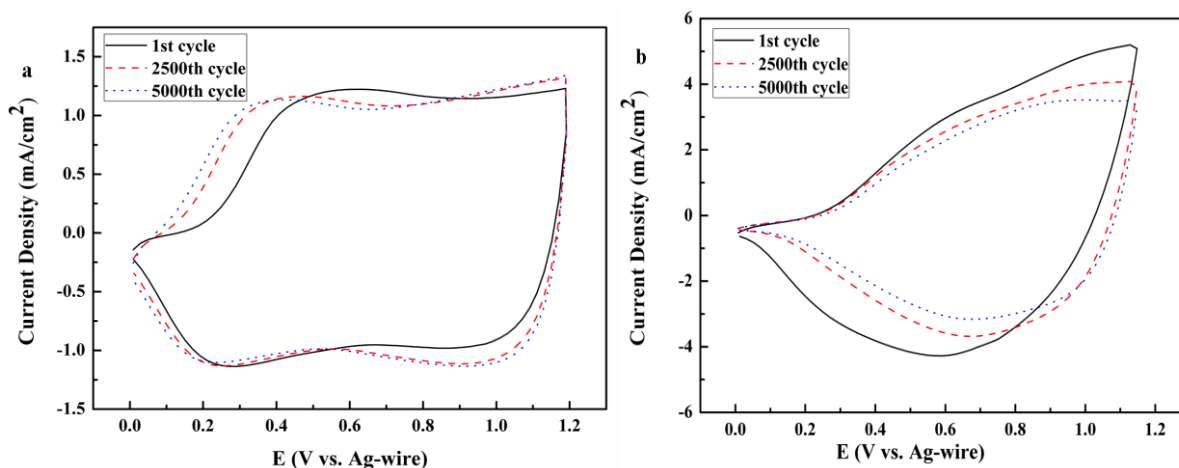


Figure 10. Stability of the polymers films cycled 5000 times with a scan rate of $100 \text{ mV} \cdot \text{s}^{-1}$ in $0.2 \text{ M TBAPF}_6/\text{ACN}/\text{DCM}$ solution. (a) CV of PDPTQ film after 1st, 2500th and 5000th cycles. (b) CV of PDPSQ film after 1st, 2500th and 5000th cycles.

The long-term switching stability was studied by the CV method, the charge losses was an indication of the stability[35]. The charge involved during the electrochemical process was calculated for each pulse period from the integration of the current. Fig.10 showed the 1st, the 2500 th and 5000 th CV curves of PDPTQ and PDPSQ, and the difference among the integrated charges was an indication of the stabilities of the polymers.

Table 2. The values of optical contrasts, switching times, CE for conjugated polymers.

	PDPTQ	PDPSQ	PDOPEQ*	PQTT*
λ^{max} (nm)	563/780/1500	636/1500	560/690/1800	440/800/1180
Optical contrasts (%)	22/27/72	28/60	29/42/90	13/12/34
Switching times (s)	1.21/0.53/0.38	0.4/0.35	-	-
CE ^a ($\text{cm}^2 \text{ C}^{-1}$)	200/71.7/218.2	210.5/366.7	-	-

^a the coloration efficiency values at corresponding dominant wavelengths.

PDOPEQ* Data were taken from Ref.³⁰

PQTT* Data were taken from Ref.²³

As shown in Fig.10a, the charge losses during the CV measurements of polymer PDPTQ were 14.41% and 24.21%, respectively, at the 2500 th and 5000 th CV curves, compared with that of the 1 st

CV curve. As for the stability of polymer PDPSQ, no any reduction in integrated charges were found even at up to 5000 th CV curves, from which it can be seen that the stability performance of PDPSQ was slightly inferior to that of PDPTQ polymer. These results indicated the good redox stability of two D-A type polymers. Considering the fact that stability tests were performed in ambient temperature environment, the decomposition of the polymers may occur by the catalysis action of environmental medium including oxygen and water. If the electrodes were sealed in fabricated devices, the long-term stability of these materials upon switching and/or cycling would be further increased.

4. CONCLUSION

In conclusion, two D-A-D type conjugated monomers were synthesized via Stille coupling reaction by employing 2,3-bis(4-(decyloxy)phenyl) quinoxaline as the acceptor unit and thiophene or selenophene as the donor unit. The corresponding polymer PDPTQ and PDPSQ were synthesized by a simple electrochemical method. The replacement of the sulfur atom by the selenium atom in the D-A-D type polymers can significantly change the optical and spectroelectrochemical properties of the polymers, including the reduction in the optical bandgap, the initial oxidation reduction potential, as well as the response time in the dynamic switching of the polymers. The difference in the electrochromic properties of two polymers might be derived from the different electron donating abilities of thiophene and selenophene, the latter has a stronger electron donating ability than that of the former. Both of the polymers have robust stability, high coloration efficiency and outstanding optical contrasts in the NIR region (72% at 1500nm for PDPTQ and 60% at 1500nm for PDPSQ). The excellent electrochemical and optical properties make these polymers good candidates for certain applications including electrochromic displays and military applications.

ACKNOWLEDGEMENTS

The work was financially supported by the National Natural Science Foundation of China (31170110, 20906043), the General and Special Program of the postdoctoral science foundation China (2013M530397, 2014T70861) and and the Natural Science Foundation of Shandong Province (ZR 2014JL009, ZR2013BQ021).

APPENDIX A. SUPPORTING INFORMATION

Supplementary data associated with this article were attached with the manuscript.

References

1. H. Shirakawa; E. J. Louis; A. G. MacDiarmid; C. K. Chiang; A. J. Heeger, *J. Chem. Soc., Chem. Commun.*, 16(1977) 578.
2. F. Würthner, *Angew. Chem. Int. Ed.* 40 (2001), 1037.
3. T. M. Swager, *Acc. Chem. Res.*, 31 (1998) 20.
4. M. D. McGehee; A. J. Heeger, *Adv. Mater.*, 12 (2000) 1655.
5. S. Holdcroft, *Adv. Mater.*, 13 (2000) 1753.

6. P. Novák, K; Müller, K; Santhanam; O. Haas, *Chem. Rev.*, 97 (1997) 207.
7. C. J. Brabec; N. S. Sariciftci; J. C. Hummelen, *Adv. Funct. Mater.*, 11 (2001) 15.
8. I. Schwendeman; J. Hwang; D. M. Welsh; D. B. Tanner; J. R. Reynolds, *Adv. Mater.*, 13 (2001) 634.
9. I. Schwendeman; R. Hickman; G. Sönmez; P. Schottland; K. Zong; D. M. Welsh; J. R. Reynolds, *Chem. Mater.*, 14 (2002) 3118.
10. K. Bange; T. Gambke, *Adv. Mater.*, 2 (1990) 10.
11. A. Pennisi; F. Simone; G. Barletta; G. Di Marco; M. Lanza, *Electrochim. Acta.*, 44 (1999) 3237.
12. D. R. Rosseinsky; R. J. Mortimer, *Adv. Mater.*, 13 (2001) 783.
13. P. Chandrasekhar; B. J. Zay; G. C. Birur; S. Rawal; E. A. Pierson; L. Kauder; T. Swanson, *Adv. Funct. Mater.*, 12 (2002) 95.
14. Y. J. Cheng; S. H. Yang; C. S. Hsu, *Chem. Rev.*, 109 (2009) 5868.
15. K. J. Albert; N. S. Lewis; C. L. Schauer; G. A. Sotzing; S. E. Stitzel; T. P. Vaid; D. R. Walt, *Chem. Rev.*, 100 (2000) 2595.
16. A. Cirpan; A. A. Argun; C. R. G. Grenier; B. D. Reeves; J. R. Reynolds, *J. Mater. Chem.*, 13 (2003) 2422.
17. A. L. Dyer; E. J. Thompson; J. R. Reynolds, *ACS Appl. Mater. Interfaces.*, 3 (2011) 1787.
18. C.M. Amb; A.L. Dyer; J.R. Reynolds, *Chem. Mater.*, 23 (2011) 397.
19. A. Durmus; G. E. Gunbas; L. Toppare, *Chem. Mater.*, 19 (2007) 6247.
20. Z. Xu; M. Wang; J. S. Zhao; C. S. Cui; W. Y. Fan; J. F. Liu, *Electrochim. Acta.*, 125 (2014) 241.
21. H. Akpınar; A. Balan; D. Baran; E. K. Ünver; L. Toppare, *Polym.*, 51 (2010) 6123.
22. S. Hayashi; T. Koizumi, *Polym. Chem.*, 3 (2012) 613.
23. S. Toksabay; S. O. Hacioglu; N. A. Unlu; A. Cirpan; L. Toppare, *Polym.*, 55 (2014) 3093.
24. E. Zhou; J. Cong, K; Hashimoto; K. Tajima, *Macromolecules*, 46 (2013)763.
25. G. A. Çetin; A. Balan; A. Durmuş; G. Günbaş; L. Toppare, *Org. Electron.*, 10 (2009) 34.
26. S. Atak; M. iÇli-Özkut; A.M. Önal; A. Cihaner, *J. Polym. Sci. Pol. Chem.*, 49 (2011) 4398.
27. C. Chen; Y. Wei; J. Lin; M. V. R. K. Moturu; W. Chao; Y. Tao; C.Chien, *J. Am. Chem. Soc.*, 128 (2006) 10992.
28. D. Keck; S. Vanderheiden; S. Bräse, *Eur. Org. Chem.*, 2006 (2006) 4916.
29. C. R. Moylan; R. D. Miller; R. J. Twieg; K. M. Betterton; V. Y. Lee; T. J. Matray; C. Nguyen, *Chem. Mater.*, 5 (1993) 1499.
30. G.E. Gunbas; A. Durmus; L. Toppare, *Adv. Funct. Mater.*, 18 (2008), 2026.
31. H. J. Chen; H. Huang; Z. F. Tian; P. Shen; B. Zhao; S. T. Tan, *Eur. Polym. J.*, 46 (2010) 673.
32. J. Zhang; Y.J.Li; Y.H.Cui; J.H.Jia; Q. Ye; L. Han; J.R. Gao, *Tetrahedron*, 71 (2015) 3802.
33. Y.X. Liu; M.Wang; J.S.Zhao; C.S.Cui; J.F.Liu, *RSC. Adv.*, 4 (2014) 52712.
34. A. Pron; P. Gawrys; M. Zagorska; D. Djurado; R. Demadrille. *Chem., Soc. Rev.*, 39 (2010) 2577.
35. Y.F.Hou, G.Q.Xu, J.S.Zhao, Y. Kong, C. Yang, *Acta. Chim. Sinica*, 12 (2014) 1238.

SUPPORTING INFORMATION

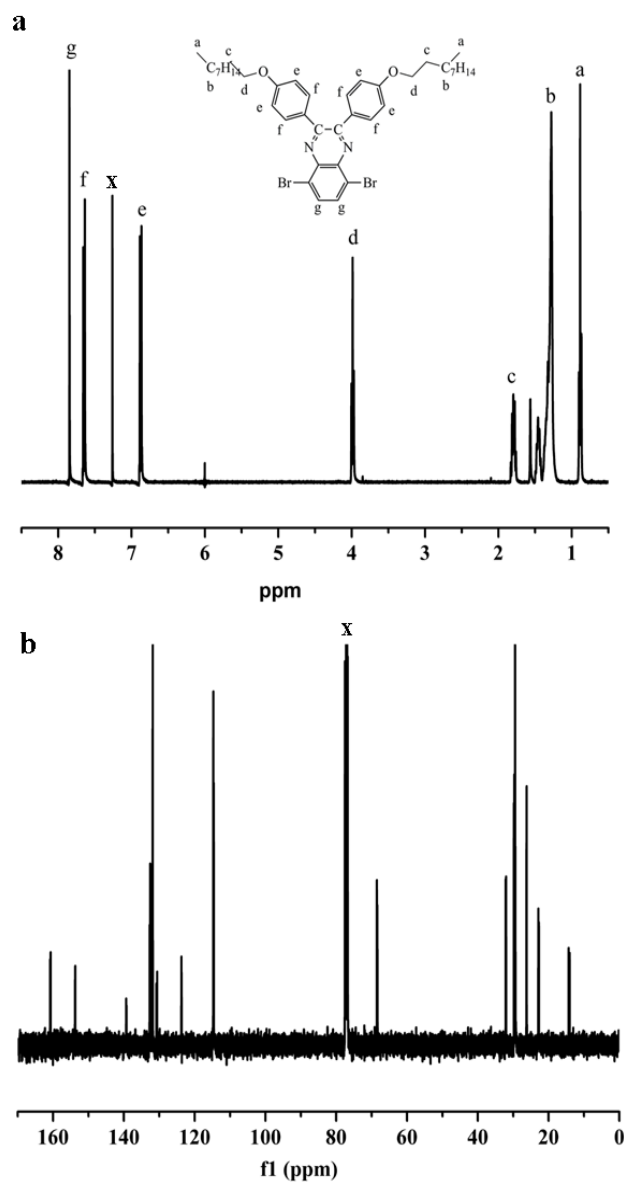


Fig. S1. (a) ¹H NMR spectrum of 5,8-dibromo-2,3-bis(4-(decyloxy)phenyl)quinoxaline in CDCl₃. Solvent peak at $\delta = 7.260$ ppm is marked by 'x'. (b) ¹³C NMR spectrum of 5,8-dibromo-2,3-bis(4-(decyloxy)phenyl)quinoxaline in CDCl₃. Solvent peak at $\delta = 77.3$ ppm is marked by 'x'.

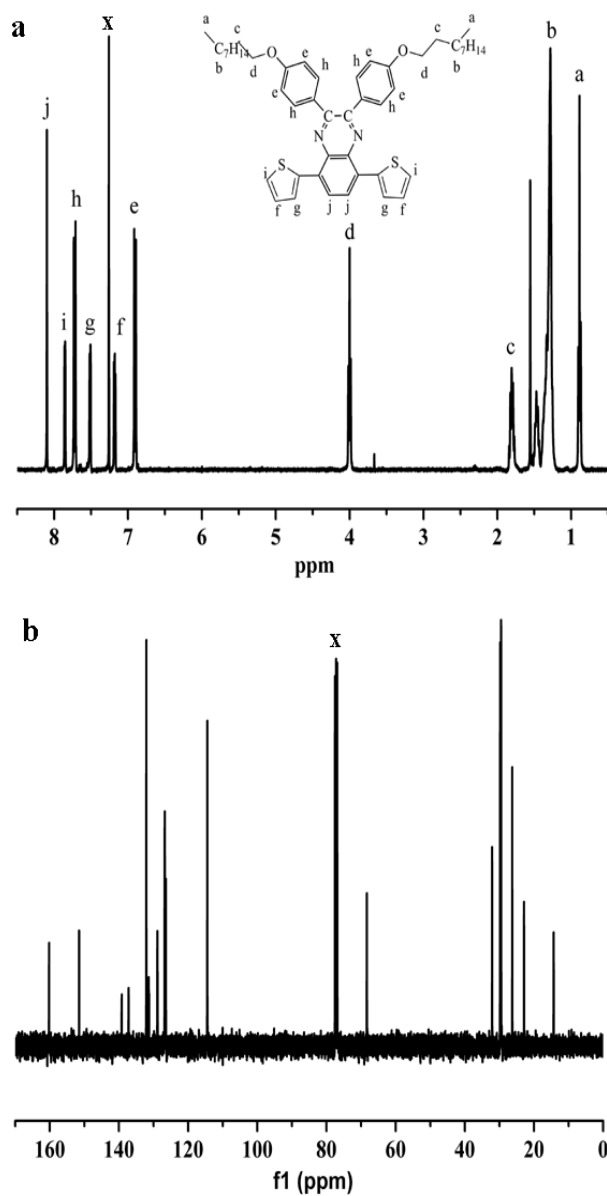


Fig. S2 (a) ^1H NMR spectrum of 2,3-bis(4-(decyloxy)phenyl)-5,8-di(thiophen-2-yl)quinoxaline (DPTQ) in CDCl_3 . Solvent peak at $\delta = 7.260$ ppm is marked by 'x'. (b) ^{13}C NMR spectrum of 2,3-bis(4-(decyloxy)phenyl)-5,8-di(thiophen-2-yl)quinoxaline (DPTQ) monomer in CDCl_3 . Solvent peak at $\delta = 77.3$ ppm is marked by 'x'.

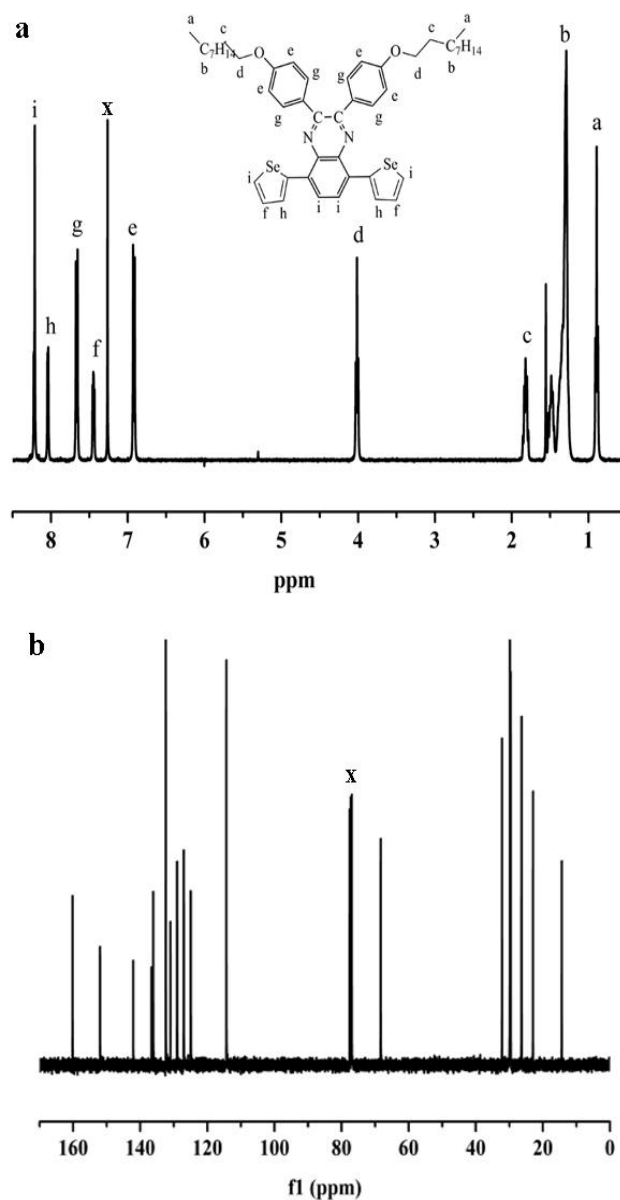


Fig. S3 (a) ¹H NMR spectrum of 2,3-bis(4-(decyloxy)phenyl)-5,8-di(selenophen-2-yl)quinoxaline (DPSQ) in CDCl₃. Solvent peak at $\delta = 7.260$ ppm is marked by 'x'. (b) ¹³C NMR spectrum of 2,3-bis(4-(decyloxy)phenyl)-5,8-di(selenophen-2-yl)quinoxaline (DPSQ) monomer in CDCl₃. Solvent peak at $\delta = 77.3$ ppm is marked by 'x'.